RSC Advances

ROYAL SOCIETY OF CHEMISTRY

www.rsc.org/advances

Eco-friendly superabsorbent composite based on sodium alginate and organo-loess with high swelling properties

Guofu MA*, Feitian Ran, Qian Yang, Enke Feng, Ziqiang Lei*

Key Laboratory of Eco-Environment-Related Polymer Materials Ministry of Education, Key Laboratory of Polymer Materials of Gansu Province, Northwest Normal University, Lanzhou 730070, China

Abstract

A novel superabsorbent composite with high swelling properties is synthesized by grafted co-polymerization partially neutralized acrylic acid (AA) onto the sodium alginate (NaAlg) backbone in the presence of organo-loess. The FTIR spectra, XRD patterns and SEM micrographs prove that the AA monomers are grafted onto the NaAlg backbone, and the organo-loess disperses in the polymer matrix which improves porous structure can be further evidenced by the element mapping. TGA and DSC results indicate that the incorporation of loess enhances the thermal stability of superabsorbent. Swelling results confirm that the proper amount of organo-loess in the superabsorbent can enhance swelling capability and salt-resistant performance. The maximum equilibrium water absorbency of the superabsorbent composite incorporated with 10 wt% organo-loess in distilled water and 0.9 wt% NaCl aqueous

Corresponding author: Key Laboratory of Eco-Environment-Related Polymer Materials Ministry of Education, Northwest Normal University, Lanzhou 730070, China. Tel.: +86 931 7975121; fax: +86 931 7975121.

E-mail address: magf@nwnu.edu.cn (G. Ma), leizq@nwnu.edu.cn (Z. Lei).

solution are 656 g g^{-1} and 69 g g^{-1}, respectively. Furthermore, the superabsorbent composite exhibits good buffer ability to external pH in the range from 4 to 10 and water retention ability. According to the performances of the eco-friendly superabsorbent composite, it can be used as a promising candidate for applications in various fields.

Keywords

Loess; superabsorbent; Swelling

1. Introduction

Superabsorbents are moderately crosslinked three-dimensional hydrophilic polymer material, which can imbibe a large amount of water or aqueous solution and display a slower water-releasing rate than traditional absorbent materials under the same conditions. That is, the superabsorbents not only have a high water absorbency but also exhibit an excellent water retention (WR) capacity.[1] Owing to their excellent properties, superabsorbents are widely used in many fileds, such as agriculture,[2,3]chemical engineering,[4] biomedical area,[5,6] tissue engineering,[7,8] waste-water treatment[9] and other environmental fields.[10,11] In general, superabsorbents include synthetic, semi-synthetic and natural polymers. Although synthetic superabsorbents have large water absorbing capacities, the consumed polymers have led to serious environmental pollution.[12] Thus, the development of eco-friendly natural-based superabsorbents incorporation of biodegradable and renewable polymers have drawn much interest owing to their abundant resources, low

production cost and good biodegradability.

Recent researches focus attention towards the superabsorbent polymers based on natural polysaccharide for their unique properties of biocompatibility, biodegradability, renewability and nontoxicity. Various polysaccharides, such as carrageenan,[13] gum ghatti,[14] chitosan,[15] guar gum[16] and alginate[17] have been investigated on hydrogel formulations. The resultant polymer exhibit quite different characteristics than the individual materials. For example, the electrical conductivity of the resultant hydrogel has much improved over that of bare hydrogel.[18] Due to these excellent properties, the polymers based on natural polysaccharides have found applications in various fields such as in agriculture, sensors, biomedical and pharmaceutical.[13,14,19] Meanwhile, much attention has also been focused on inorganic clay materials for preparing superabsorbent composites, owing to the environmental advantages and practical applications. Clays, including kaolin,[20] vermiculite,[21] attapulgite,[17] montmorillonite,[22] muscovite[23] and rectorite[12] have already been incorporated into poly(acrylic acid) and polyacrylamide polymeric network to reduce production costs, improve the network structure and properties of superabsorbents, as well as accelerate the generation of new materials for special application.[24]

Sodium alginate (NaAlg) is a linear chained anionic natural polysaccharide composed of 1,4-linked β-D-mannuronic acid (M block units) and α-L-guluronic acid (G block units) which are arranged in an irregular blockwise pattern of various proportions of GG, MG, and MM blocks (Scheme 1).[25] And the NaAlg is renewable,

abundant, nontoxic, water-soluble, biodegradable and biocompatible, because it is generally extracted from various species of brown algae. It has plentiful free hydroxyl and carboxyl groups distributed along the backbone, which can be easily crosslinked with other multivalent cations such as calcium or organic crosslinker like glutaraldehyde,[26] grafted co-polymerization with hydrophilic vinyl monomers, polymer blending and compounding with other functional components.[27] The above properties make it ideal for industrial applications.

Loess is a type of hydrous magnesium aluminum silicate with reactive hydroxyl groups on its surface. Due to its hydrophilic property, abundant reserves and extremely low prices, loess is an ideal inorganic component to improve the network structure and swelling property. Organic-modified loess with quaternary ammonium salt can change the surface properties and render hydrophilic silicate, thereby resulting in the alteration of adhesion and dispersing performances of loess in polymer matrix.[28] Inherent advantages of inorganic component and the strong interfacial interactions between the dispersed loess and the polymer matrix enhance the thermal stability as well as swelling and adsorption behavior of the virgin polymer.[23] To the best of our knowledge, there has been a few reports about the preparation of superabsorbent based on natural loess clay, even no literature about that based on organo-loess. Therefore, the introduction of organo-loess in superabsorbent is expected to provide a new method to extend the utilization of loess, reduce the cost and improve the biocompatibility and biodegradability of the superabsorbent.

As a further study for organic-inorganic compound superabsorbents, our target focuses on providing new strategies for the high-value utilization of cheap natural loess and sodium alginate, improving swelling properties and reducing production cost of corresponding superabsorbents. Incorporation of biodegradable and renewable natural polysaccharide (NaAlg) can improve biodegradability of corresponding superabsorbent materials, as well as reduce the dependence on petrochemical derived monomers. In this study, a novel and eco-friendly superabsorbent composite were prepared by grafted co-polymerization partially neutralized acrylic acid (AA) onto the sodium alginate (NaAlg) backbones in the presence of organo-loess in aqueous solution. The composite was characterized by Fourier transform infrared (FTIR) spectroscopy, X-ray diffraction (XRD), scanning electron microscopy (SEM), element mapping and Thermogravimetric analysisnalysis (TGA) and DSC. The effects of organo-loess on the water absorption abilities in distilled water and 0.9 wt% NaCl solutions were discussed. Furthermore, the factors such as pH value, surfactants and salines that could affect the swelling ratio of superabsorbent composites and water retention capacity were also systematically investigated.

2. Experimental

2.1 Materials

Loess was collected from WuQuan mountain in Lanzhou city, Gansu province, China, Sodium alginate (NaAlg, Shanghai chemical reagents Co., China, average molecular weight 500,000 and degree of deacetylation 84%), acrylic acid (AA, analytical grade,

Tianjin Kaixin Chemical Industrial Co., China), ammonium persulfate (APS, analytical grade, Yantai Shuangshuang Chemical Industrial Co., China), N,N-methylenebisacrylamide (MBA, chemically pure, Sinopharm Chemical Reagent Co., China), sodium dodecyl benzene sulfonate (SDBS, analytical grade, Sinopharm Chemical Reagent Co., China), cetyltrimethyl ammonium bromide (CTAB, analytical grade, Shanghai Chemical Reagent Co., China). All other reagents used were of analytical grade and all solutions were prepared with distilled water.

2.2 Preparation of organo-loess

Organo-loess was prepared as follows: 10.0 g loess purified by suspension method was immersed in 100 mL distilled water in 250 mL flask and heated for 30 min at 1250 rpm stirring. Then 1.0 g of CTAB was added into the flask. The mixture was stirred vigorously at 85^{o}C for 90 min. Then the product was washed and filtrated repeatedly until no Br^- was detected by 0.1mol/L $AgNO_3$ aqueous solution in the filtrate. The product was dried for several hours to constant weight at 60^{o}C on an oven and then milled to 320 mesh size for further use.

2.3 Preparation of superabsorbent composites

A series of superabsorbent composites with different amounts of organo-loess were prepared according to the following procedure. 1.2 g of NaAlg was dissolved in 30 mL distilled water in a 250 mL four-necked flask equipped with mechanical stirrer, reflux condenser, a constant pressure dropping funnel and a nitrogen line. The obtained viscous solution was heated to 60^{o}C in an oil bath for 1 h to form

homogeneous colloidal slurry. Then, an aqueous solution of initiator APS (0.100 g in 5 mL H_2O) was added and kept at 60°C for 15 min to generate radicals. After cooling the reactants to 40°C, 17 ml of the mixed solution containing 7.2 g of AA neutralized with 8.5 ml of NaOH solution (8.0 mol/L), 0.02 g of crosslinker MBA and a calculated amounts of organo-loess (0, 0.45, 0.95, 1.5, 2.15 g) were added to the reaction flask. The reaction temperature was slowly risen to 70°C and maintained for 3 h to complete polymerization. A nitrogen atmosphere was maintained throughout the reaction period. The obtained samples were spread on a dish to dry to a constant weight at 60°C in an oven. The dry samples were milled and all samples used for test had a particle size in the range of 20-50 mesh (230-870 μm). Scheme 2 represents the general procedure for the preparation of NaAlg-g-PAA/organo-loess superabsorbent composites.

For comparison purpose, the NaAlg-g-PAA and NaAlg-g-PAA/loess composites were prepared under the same condition.

2.4 Measurements of equilibrium water absorbency

Measurements of equilibrium water absorbency were performed at room temperature according to a conventional filtration method.[29] A weighted quantity of the superabsorbent composite (0.10 g) with particle sizes between 20 and 50 mesh (230-870 μm) was immersed in 250 mL distilled water or 100 mL 0.9wt % NaCl solution. The samples were allowed to absorb water at room temperature for 4 h to reach swelling equilibrium. Then, the swollen samples were taken out from excess

water by filtering through a 100-mesh screen under gravity for 10 min until no redundant water can be removed. After weighing the swollen samples, the equilibrium absorbency (Q_{eq}) of the samples was calculated using the following formula:

$$Q_{eq} = \frac{m_2 - m_1}{m_1} \quad (1)$$

Where m_2 and m_1 are the weights of swollen gel and the dried sample, respectively. Q_{eq} was calculated as grams of water per gram of sample.

The determination of water absorbencies at various pH solutions was similar to that of above measurement. The pH values of the external solution were adjusted using 0.1 mol/L HCl and 0.1 mol/L NaOH solutions. The effects of various pH solutions on water absorbency can then be achieved. All samples were carried out three times repeatedly and the average values were reported in this paper.

2.5 Measurements of water absorbency in various saline solutions

Accurately weighed 0.10 g sample was immersed in 250 mL of various saline (NaCl, $CaCl_2$, $FeCl_3$) solutions with different concentrations for 4 h to maintain equilibrium. The swollen samples were filtered through a 100-mesh screen and weighted. The water absorbency in various saline solutions could then be calculated using the formula (1).

2.6 Measurements of water absorbency in surfactant solutions

Water absorbency in different surfactant solutions with various concentrations was determined according to the above method described in section 2.5.

2.7 Measurement of water retention (*WR*)

The determination of the water retention was carried out according to the following procedure.[30] Accurately weighed 30 g fully swollen samples were spread in the bottom of a 250 mL beaker and placed into an oven at 60 and 100°C, respectively. The weight of the swollen samples was determined every 1 h. *WR* was calculated according to the following formula.

$$WR = \frac{W - W_d}{W_0 - W_d} \times 100\% \quad (2)$$

Where W_0 is the weight of the fully swollen sample， W_d is the weight of the dry sample and W is the weight of the sample heated for different times at certain temperature.

2.8 Characterization

FTIR measurements were performed on a FTIR-FTS3000 spectrometer. The samples were completely dried before measurement. All spectra collected 40 scans over a wavenumber of 400-4000 cm^{-1} at 8 cm^{-1} resolution were obtained from compressed KBr pellets in which the samples concentration of about 3%. The morphologies of the superabsorbent composites were examined using a field emission scanning electron microscope (FESEM, Carl Zeiss Ultra plus, Germany) with an acceleration voltage of 3 kV. Before the SEM observation, the samples were completely dried and coated with a thin layer of gold. The element mapping was carried out using the Elemental Analyzer Vario EL. X-ray diffraction (XRD) of samples was performed using a Rigaku D/Max-2400 diffractometer with Cu Kα radiation (k =1.5418 Å) at 40 kV, 100 mA, scanning from 3° to 80° at 5°/min. Thermogravimetric analysis (TGA) and DSC

of synthesized composites have been recorded on TGA/DSC1 analyzer (Mettler Toledo) at a heating rate of 10°C/min under nitrogen.

3. Results and discussion

3.1 FTIR spectra analysis

The FTIR spectra of (a) loess and (b) organo-loess are shown in Fig. 1. As can be seen, the main characteristic absorption bands of loess at 3619 cm^{-1}, 3455 cm^{-1}, 1622 cm^{-1}, 1024 cm^{-1}, 692 cm^{-1} and 468 cm^{-1} are ascribed to –OH stretching, bending of –OH, Si–O asymmetric stretching, Si–O–Si symmetric stretching, and bending of Si–O (Fig. 1a), respectively.[31] Compared with the spectrum of organo-loess, the new adsorption peaks at 2919 cm^{-1} and 2851 cm^{-1} can be found, which are ascribed to asymmetric and symmetric stretching vibration of C–H bonds of alkylammonium chain appeared (Fig. 1b), indicating organic cations of CTAB had been exchanged with loess.[32]

The FTIR spectra of (a) NaAlg, (b) NaAlg-g-PAA, (c) NaAlg-g-PAA/loess, (d) NaAlg-g-PAA/organo-loess are shown in Fig. 2. As can be seen, the characteristic absorption bands of NaAlg at 1093 and 1031 cm^{-1} (stretching vibration of C–OH groups) are weakened after reaction, which indicate the –OH groups of NaAlg has participated in chemical reaction. The new bands at 1559 cm^{-1} for NaAlg-g-PAA and 1556 cm^{-1} for NaAlg-g-PAA/organo-loess (asymmetric stretching vibration of $–COO^-$ groups), and at 1456 and 1411 cm^{-1} (symmetric stretching vibration of $–COO^-$ groups) are observed in the spectra of NaAlg-g-PAA and NaAlg-g-PAA/organo-loess (Fig. 2b, d), which indicate that PAA chains have been grafted onto the NaAlg backbone.[27] The

bands at 1569 and 1457-1410 cm^{-1} are assigned to the asymmetric and symmetric stretching vibration of the –COO^- groups, respectively. The –OH absorption bands of organo-loess at 3620 cm^{-1} can almost not be observed, and the Si–O absorption band at 1024 cm^{-1} shifted to 1031 cm^{-1} with a weakened intensity (Fig.1b and Fig. 2d). The above information confirm that loess and organo-loess have participated in co-polymerization reaction by its active silanol groups.[33]

3.2 Morphology analysis

The scanning electron micrographs (SEM) of (a) NaAlg-g-PAA, (b) NaAlg-g-PAA/loess and (c) NaAlg-g-PAA/organo-loess with 10 wt% loess (organo-loess) are presented in Fig. 3. As indicate in Fig. 3, the fracture surface morphology of the NaAlg-g-PAA (Fig. 3a) is different from that of NaAlg-g-PAA/loess (Fig. 3b) and NaAlg-g-PAA/organo-loess (Fig. 3c). It can be observed that the NaAlg-g-PAA (Fig. 3a) display a relatively smooth and tight surface. However, the composites containing the loess or organo-loess have undulant, coarse and crapy surface (Fig. 3b and Fig. 3c). However, comparing with the incorporation loess into the composites, the organo-loess make the pores become smaller and the loess is dispersed more uniformly. This can be attributed to the fact that the long alkyl chains of CTAB can reduce the interaction between hydrophilic groups and enhance the compatibility of loess with the polymeric matrix.[34] This fracture surface morphology change is attributed to the introduction of loess, and then may have some influence on water permeation regions and swelling behaviors of the corresponding

superabsorbent composites.

By contrast with NaAlg-g-PAA, NaAlg-g-PAA/organo-loess was further characterized by element mapping images of carbon, oxygen, magnesium, aluminum and silicon to analyze the elemental distribution (Fig. 4). Fig. 4 suggeste that magnesium, aluminum and silicon are distributed evenly in carbon and oxygen. That is to say, loess has been distributed in NaAlg-g-PAA polymeric matrix evenly, because the major ingredient of loess is magnesium, aluminum and silicon.

3.3 XRD analysis

The reaction between loess and NaAlg-g-PAA were also investigated by XRD. Fig. 5 displays XRD patterns of the (a) loess, (b) organo-loess, (c) NaAlg-g-PAA/loess and (d) NaAlg-g-PAA/organo-loess superabsorbent composites. The diffraction peaks of loess are observed at $2\theta = 8.78°$ (d = 10.06 Å), $2\theta = 19.66°$ (d = 4.51 Å) and $2\theta = 26.56°$ (d = 3.35 Å), which can be attributed to the characteristic diffraction of mica, quartz and sanidine, respectively. The peaks at $2\theta = 12.38°$ (d = 7.14 Å) and $2\theta = 21.96°$ (d = 4.04 Å) can be attributed to the characteristic diffraction of kaolinite. The above results indicate the main mineral components of the loess are mica, quartz, sanidine and kaolinite.[29] After being organified, the positions of diffraction peaks of loess had no changes, suggesting that CTAB does not intercalate into the interlayers of loess and is only adsorbed on the surface of loess. However, in the XRD pattern of NaAlg-g-PAA/loess and NaAlg-g-PAA/organo-loess superabsorbent composites, most of characteristic diffraction peaks of loess can not be detected and the diffraction

peak of loess at 2θ = 26.56° (d = 3.35 Å) has been shifted toward a lower angle at 2θ = 26.42° (d = 3.37 Å). This results indicate that the majority of loess and organo-loess have been exfoliated and dispersed uniformly in the polymer matrix which should have interacted on the surface of loess rather than be incorporated into the interlayer spacing.

3.4 Thermal stability analysis

The effect of introducing loess on the thermal stability of the synthesized superabsorbent composite was investigated using TGA technique. It can be observed from Fig. 6, the NaAlg-g-PAA, NaAlg-g-PAA/loess (10 wt%) and NaAlg-g-PAA/organo-loess (10wt%) exhibit three-stage thermal decomposition processes, and the weight loss rate of NaAlg-g-PAA is obviously faster than NaAlg-g-PAA/loess and NaAlg-g-PAA/organo-loess. At the initial stage, the weight loss about 20.1% from 29.5 to 291^{o}C (for NaAlg-g-PAA) and about 18.8% from 29.1 to 307.2^{o}C (for NaAlg-g-PAA/organo-loess) may correspond to the loss of adsorbed and bound water. The weight loss about 30% between 291 and 431^{o}C for NaAlg-g-PAA is attributed to the dehydration of saccharide rings, the breaking of C–O–C bonds in the chain of NaAlg and the elimination of the water molecule from the two neighboring carboxylic groups of the polymer chains due to the formation of anhydride[23]. However, this process is delayed and showed a weight loss of 14.4% in the temperature range of 306-410.6^{o}C for NaAlg-g-PAA/organo-loess. The successive weight loss about 20.3% from 406 to 800^{o}C for NaAlg-g-PAA and about 30.8% in the

range of 411.5-800°C for NaAlg-g-PAA/organo-loess can be attributed to the destruction of carboxylic groups and CO_2 evolution, main chain scission and the breakage of crosslinked network structure[32]. Based on the above information, it can be found that NaAlg-g-PAA/loess and NaAlg-g-PAA/organo-loess show lower weight loss rate and smaller total weight loss comparing with NaAlg-g-PAA, which indicate that the incorporation of loess is helpful to improve the thermal stability of NaAlg-g-PAA. This result is attributed to effects such as a decrease in permeability due to "tortuous path" effect of loess that delays the permeation of oxygen and the escape of volatile degradation products.[15] Similar clay effect on thermal resistance of hydrogel composites was also reported in literature[29].

3.5 DSC analysis

The DSC curves of NaAlg-g-PAA, NaAlg-g-PAA/loess (10 wt%) and NaAlg-g-PAA/organo-loess (10 wt%) are given in Fig 7. It can be observed that NaAlg-g-PAA show an endothermic peak at 72ºC and an exothermic peak at 210ºC, whereas NaAlg-g-PAA/loess composite show an endothermic peak at 77ºC and an exothermic peak at 223ºC. The initial peak at 77ºC corresponds to oxidation of water contents.[35] Compared with NaAlg-g-PAA, the glass transition temperature (*Tg*) of composite incorporated in loess tends to move to higher values. This phenomenon can be explained by the coupling model theory, the segmental motion of polymers below *Tg* is cooperative process and had to overcome the resistance from the surrounding segments in order to accomplish the transformation between configurations. As more

segments are restricted by the presence of loess, the activation threshold for the motion of some segments became higher.[36] As a consequence, NaAlg-g-PAA/loess and NaAlg-g-PAA/organo-loess have exhibited a higher *Tg* than NaAlg-g-PAA. In addition, the glass transition temperature of a cross-linked polymer is proportional to the effective cross-link chain density. The above results indicate that the synthesized superabsorbent composites have well cross-link density[37].

3.6 Effect of loess content on water absorbency

The water absorbencies of NaAlg-g-PAA/loess and NaAlg-g-PAA/organo-loess series superabsorbent composites in distilled water and 0.9 wt% NaCl aqueous solutions are presented in Fig. 8. The content of loess is an important influencing factor on the water absorbencies of the superabsorbent composites. The water absorbencies of the NaAlg-g-PAA/loess and NaAlg-g-PAA/organo-loess composites all increased with increasing the content of loess or organo-loess when the content of them are lower than 10 wt%. This tendency may be due to the fact that loess powder participated in the formation of three-dimensional network structure, and the introduction of loess greatly decrease the hydrogen bonding interaction among hydrophilic groups and restrained the entanglement of polymer chains, thus the physical crosslinking degree is decreased.[27] As a result, the swelling capacity can be evidently enhanced. However, with further increasing content of loess or organo-loess from 10 to 20 wt%, more crosslinking points are generated, which decrease elasticity of polymer chains. Additionally, the excess of loess also decrease the hydrophilicity as well as the

osmotic pressure difference, resulting in the decrease of water absorbency.[22] The highest water absorbency for the composite incorporated with 10 wt% organo-loess is 656 g g^{-1} in distilled water and 69 g g^{-1} in 0.9 wt% NaCl solution, respectively. Furthermore, the changes of water absorbencies for the introduction of organo-loess are more obvious than the introduction of loess both in distilled water and in 0.9 wt% NaCl solutions in the range of loess content investigated. This phenomenon may be attributed to the fact that the organo-loess improve the polymeric network to a higher extent, comparing with that of the doped with loess. The loess is exchanged by the CTBA ion and the long alkyl chains of CTBA attached onto the surface of loess microparticles, which improve the polymeric network by forming tiny hydrophobic regions, and also weakene the hydrogen bonding interaction among hydrophilic groups.[38]

These results reveale that the incorporation of moderate amount of loess into polymer matrix can enhance the water absorbencies of the superabsorbent as well as reduce its dependence on petrochemical-derived monomers. This will provide a novel way for producing low-cost and eco-friendly superaborbent materials, and make it has a great potential for applications in the fields of agriculture and horticulture.

3.7 Effect of cross-linking density on water absorbency

The cross-linking density of the hydrogel network in the synthesized composites is an important swelling control factor and depends upon the amount of crosslinking agent used. In the present work, the variation of MBA amount (0.016-0.024 g) were

investigated according to water absorbencies of superabsorbent composites (Fig. 9). The water absorbency increased with the increasing the content of crosslinking agent from 0.016 to 0.02 g and the maximum water absorbency is achieved when the amount of crosslinking agent is 0.02 g. This phenomenon is due to the fact that amount of soluble material increased and three-dimensional network of the superabsorbent composites can not be formed efficiently when the amount of crosslinking agent is lower than 0.016 g, which result in a samller swelling ratio of the superabsorbent composites. When the amount of crosslinker increased and exceed 0.02 g, more crosslink points are produced during polymerization and cause the higher cross-linking density and decrease the space of polymer three-dimensional network, and consequently, it will not be beneficial to expand the structure and hold a large quantity of water.[18,22]

3.8 Effect of various pH solutions on swelling behaviors

The swelling behaviors of NaAlg-g-PAA, NaAlg-g-PAA/loess (10 wt% loess) and NaAlg-g-PAA/organo-loess (10 wt% organo-loess) superabsorbent composites are investigated in various pH solutions ranged from 2 to 12 (Fig. 10). The solution pH was adjusted by NaOH (pH=13.0), HCl (pH=1.0) and distilled water to reach the desired value. The water absorbencies for all testing samples drastically increased at the pH range from 2 to 4 and decreased at the pH range from 10 to 12. This is because most of the $–COO^-$ groups change into –COOH groups when the pH<4, the repulsion between polymeric chains decreased, which led to the decrease of water absorbency.

When the pH>10, most of the –COOH groups changed into $–COO^-$ groups, and the screening effect of the counterion (Na^+) on the poly-anionic chain is more evident, which also led to a decrease of the water absorbency. This phenomena imply that the buffer action of –COOH and $–COO^-$ has disappeared when a large amount of acid or base is added.[39] However, the equilibrium water absorbencies keep roughly constant in the pH range from 4 to 10. This can be attributed to the fact that some of carboxylate groups are ionized and the ionization degree of the carboxylate groups keeps almost constant, which induce a similar osmotic pressure between the hydrogel network and the external solution as well as the electrostatic repulsion among the $–COO^-$ groups.

In addition, the hydrogen bonding interactions among the –COOH groups is partially broken due to the introduction of organo-loess or loess, which widene the mesh size of the network pores and thus enhance the swelling capacity in a wide range of pH values.[21] Based on the above analyses, the superabsorbent composites are very advantageous for use of various soils for agricutural application.

3.9 Effects of saline solutions on swelling behaviors

The effect of saline solutions on the swelling properties of superabsorbents is significant to the expanding of their practical applications especially for agriculture and horticulture. In current section, the influence of saline solution (NaCl, $CaCl_2$, $FeCl_3$) with various concentration on the swelling properties of NaAlg-g-PAA, NaAlg-g-PAA/loess (10 wt% loess) and NaAlg-g-PAA/organo-loess (10 wt%

organo-loess) composites were investigated (Fig. 11a, b, c). It indicate the swelling capacity at equilibrium decreased as the concentration of external saline solutions increased. The reason may be that the increasing saline concentration led to the reduction of the osmotic swelling pressure difference between the polymer matrix and the external solution which prevente water molecules to penetrate inside the hydrogels.[40] It also can be seen that equilibrium swelling capacity of these superabsorbent composites in various saline solutions of the same concentration are all in the order NaAlg-g-PAA < NaAlg-g-PAA/loess < NaAlg-g-PAA/organo-loess. This tendency can be explained by the fact that loess is insensitive to saline solution and enhance osmotic pressure difference between the polymeric network and external saline solutions. Comparing with NaAlg-g-PAA/loess, the higher swelling capacity for NaAlg-g-PAA/organo-loess composite in various saline solutions may be due to the fact that the long alkyl chains of organo-loess has interfered the formation of complex between carboxylate groups and cations.[38] Additionally, the swelling capability of all samples in NaCl solution is higher than theirs in $CaCl_2$ and $FeCl_3$ solutions. This result is mainly caused by the complexing ability difference of the carboxylate group on the superabsorbent network to various cations. The order of the ability of the carboxylate group to form a complex with the three cations is Na^+ < Ca^{2+} < Fe^{3+}, based on their formation constants for ethylenediamine tetraacetic acid (EDTA).[41] These results obtained indicated that the introduction of organo-loess or loess can improve salt-resistant property of the corresponding superabsorbent

composites.

3.10 Effects of surfactant solutions on swelling behaviors

To investigate the influence of ionic surfactants on the equilibrium swelling behaviors, the swelling behaviors of NaAlg-g-PAA/loess (10 wt% loess) and NaAlg-g-PAA/organo-loess (10 wt% organo-loess) superabsorbent composites in SDBS and CTAB solutions with various concentrations were explored, respectively (Fig. 12). The swelling capacity of two kinds of testing samples all decreased with increasing the concentration of SDBS and CTAB solutions. This behavior is attributed to the differences in the counterions, the ionizable groups and the bound amounts of surfactants.[42] However, the decreasing trend in the CTAB solution is more obvious than in the SDBS solution. This may be due to the strong association, binding or interaction of cationic surfactant molecules with the counter ions or ionizable groups of hydrogels as well as aggregation of the surfactant molecules within or over the networks of hydrogels.[43] These factors are responsible for the rapid decreasing rate and low swelling capacity of the composites in the CTAB solution. In the anionic surfactant SDBS solution, owing to the repulsion of the negatively charged $–COO^-$ groups with the anions of the polymeric chains, the DBS^- moieties barely entered the network of the composite.[44] Consequently, the superabsorbent composites exhibite comparatively higher swelling capacity in the anionic surfactant solution than in the cationic surfactant solution

3.11 Water retention ability

Water retention ability is an important factor for the application of a superabsorbent in practice. The water retention ability of fully swollen NaAlg-g-PAA/loess containing 10% loess and NaAlg-g-PAA/organo-loess containing 10% organo-loess superabsorbent composite at different temperatures (40 and 100^{o}C) were explored (Fig. 13). The results indicate that the water retention ability had a decreasing tendency with prolonging the time and water retention curve at 40^{o}C is flat than at 100^{o}C. Moreover, the water retention ability of two kinds of superabsorbents is very close, and it is more than 69% after 12 h at 40 and 100^{o}C, it also can keep approximately 8 h, respectively. This indicate the superabsorbent composites have excellent water retention ability and are expected to have a great potential application for agriculture and horticulture, especially for saving water in dry and desert regions.

4. Conclusions

A novel organic-inorganic superabsorbent composite was successfully synthesized by incorporating organo-loess or loess into the NaAlg-g-PAA polymeric network in aqueous solution. The FTIR and XRD confirmed that AA had been grafted on to NaAlg backbones, organo-loess and loess participated in co-polymerization reaction. SEM and element mapping observation revealed that the surface structure of the superabsorbent composites was improved and organo-loess led to a better dispersion. TGA and DSC results indicated that the incorporation of loess improved the thermal stability of superabsorbent. The superabsorbent composites exhibited excellent water absorbencies and water retention abilities, and the maximum equilibrium water

absorbency in distilled water and 0.9 wt% NaCl aqueous solutions were 656 g g^{-1} and 69 g g^{-1}, respectively. Swelling measurements indicated that superabsorbent composites had good buffer ability to external pH in the range from 4 to 10, and higher swelling capacity in anionic surfactant (SDBS) than that of cationic surfactant (CTAB) solution. The impact of external saline solutions on the swelling capacity has the following order: $Na^+ < Ca^{2+} < Fe^{3+}$. Based on above description, we can conclude that the incorporation of suitable amount of loess or organo-loess into the NaAlg-g-PAA polymeric network could not only enhance the swelling capacity of the composites but also improve the buffer ability to external pH and salt-resistant ability, and that of doped with organo-loess is more obvious comparing with that of doped with loess, which is an effective approach to improve the performance and extend the application of superabsorbent composite such as drug delivery, hygienic products, agriculture and horticulture.

Acknowledgements

We thank to the National Natural Science Foundation of China (NO.21164009), the program for Changjiang Scholars and Innovative Research Team in University (IRT1177), Key Laboratory of Eco-Environment-Related Polymer Materials (Northwest Normal University) of Ministry of Education, and Key Laboratory of Polymer Materials of Gansu Province.

References

1. M. Zhang, Z. Cheng, M. Liu, Y. Zhang, M. Hu and J. Li, *J. Appl. Polym. Sci.*, 2014,

131. DOI: 10.1002/APP.40471.

2 M. R. Guilherme, A. V. Reis, A. T. Paulino, T. A. Moia, L. H. Mattoso and E. B. Tambourgi, *J. Appl. Polym. Sci.*, 2010, **117**, 3146-3154.

3. R. Meena, M. Chhatbar, K. Prasad and A. K. Siddhanta, *Polym. Int.*, 2008, ***57***, 329-336.

4. G. Jiang, C. Liu, X. Liu, Q. Chen, G. Zhang, M. Yang and F. Liu, *Polymer*, 2010, **51**, 1507-1515.

5. P. K. Murthy, Y. Murali Mohan, K. Varaprasad, B. Sreedhar and K. Mohana Raju, *J. Colloid. Interf. Sci.*, 2008, **318**, 217-224.

6. T. S. Anirudhan and S. R. Rejeena, *J. Appl. Polym. Sci*., 2014, **131**, 40699-40711.

7. F. Brandl, F. Sommer and A. Goepferich, *Biomaterials*, 2007, **28**, 134-146.

8. X. Wang, S. P. Strand, Y. Du and K. M. Vårum, *Carbohyd. Polym.*, 2010, **79**, 590-596.

9. W. Kangwansupamonkon, W. Jitbunpot and S. Kiatkamjornwong, *Polym. Degrad. Stabil*., 2010, **95**, 1894-1902.

10. Y. Zheng and A. Wang, *J. Hazard. Mater.*, 2009, **171**, 671-677.

11. R. Tankhiwale and S. K. Bajpai, *Colloid. Surface B.*, 2009, **69**, 164-168.

12. L. Yang, X. Ma, N. Guo and Y. Zhang. *Carbohyd. Polym.*, 2014, **105**, 351-358.

13. G. R. Mahdavinia, H. Etemadi and F. Soleymani. *Carbohyd. Polym.*, 2015, **128**, 112-121.

14. K. Sharma, V. Kumar, B. S. Kaith, V. Kumar, S. Som, S. Kalia and H. C. Swart, *Polym. Degrad. Stabil.*, 2015, **111**, 20-31.

15. H. Ferfera-Harrar, N. Aiouaz, N. Dairi and A. S. Hadj-Hamou, *J. Appl. Polym. Sci.*, 2014, **131**(1). DOI: 10.1002/app.39747.

16. W. Wang, J. Zhang and A. Wang, *Appl. Clay. Sci.* 2009, **46**, 21-26.

17. Y. Wang, W. Wang, X. Shi and A. Wang, *Polym. Bull.*, 2013, **70**, 1181-1193.

18. B. S. Kaith, K. Sharma, V. Kumar, S. Kalia and H. C. Swart, *Synthetic Met.*, 2014, **187**, 61-67.

19. K. Sharma, V. Kumar, B. S. Kaith, S. Som and V. Kumar, *Ind. Eng. Chem. Res.*, 2015, **54**(7), 1982-1991.

20. H. Zhu and X. Yao, *J. Macromol. Sci. A.*, 2013, **50**, 175-184.

21. X. Shi, W. Wang and A. Wang, *J. Compos. Mater.*, 2011, **45**, 2189-2198.

22. S. Zhang, Y. Guan, G. Q. Fu, B. Y. Chen, F. Peng, C. L. Yao and R. C. Sun, *J. Nanomater.*, 2014, **2**. DOI: org/10.1155/2014/675035.

23. T. Wan, Z. Zhou, R. Huang, C. Zou, M. Xu, W. Cheng and R. Li, *Appl. Clay Sci.* 2014, **101**, 199-204.

24. D. Gao, R. B. Heimann, J. Lerchner, J. Seidel and G. Wolf, *J. Mater. Sci.* 2001, **36**, 4567-4571.

25. S. Bekin, S. Sarmad, K. Gürkan, G. Keçeli and G. Gürdağ, *Sensor. Actuat. B-Chem.* 2014, **202**, 878-892.

26. H. S. Samanta and S. K. Ray, *Carbohyd. Polym.*, 2014, **99**, 666-678.

27. W. Wang and A. Wang, *Carbohyd. Polym*., 2010, **80**, 1028-1036.

28. J. Wang, Q. Wang, Y. Zheng and A. Wang, *Polym. Composite*, 2013, **34**, 274-281.

29. M. Irani, H. Ismail and Z. Ahmad, *J. Appl. Polym. Sci.*, 2014, **131**, 40101-40111.

30. X. Qi, M. Liu, Z. Chen and R. Liang, *Polym. Advan. Technol.*, 2007, **18**, 184-193.

31. Q. Tang, J. Lin, J. Wu, Y. Xu and C. Zhang, *J. Appl. Polym. Sci.* 2007, **104**, 735-739.

32. Y. Xie and A. Wang, *J. Compos. Mater.*, 2009, **43**, 2401-2417.

33. X Shi, W Wang, Y. Kang and A. Wang, *J. Appl. Polym. Sci.*, 2012, **125**, 1822-1832.

34. Y. Wang, W. Wang and A. Wang, *Chem. Eng. J.*, 2013, **228**, 132-139.

35. S. Menon, M. V. Deepthi, R. R. N. Sailaja and G. S. Ananthapadmanabha, *Indian Journal of Advances in Chemical Science*, 2014, **2**(2), 76-83.

36. X. Xia, X. Zeng, J. Liu and W. Xu, *J. Appl. Polym. Sci*., 2010, **118**(4), 2461-2466.

37. Y. Xiang, Z. Peng and D. Chen, *Eur. Polym. J*., 2006, **42**(9), 2125-2132.

38. J. Zhang, H. Chen and A. Wang, *Eur. Polym. J.*, 2005, **41**, 2434-2442.

39. Zhang J, Li A and Wang A. *Polym. Advan. Technol.*, 2005, **16**, 813-820.

40. Y. Zhou, S. Fu, L. *Carbohyd. Polym.* 2013, **97**, 429-435.

41. J. Zhang, H. Chen and A. Wang, *Polym. Advan. Technol.*, 2006, **17**, 379-385.

42. T. Caykara and G. Birlik, *Macromol. Mater. Eng.*, 2005, **290**, 869-874.

43. Y. M. Mohan, T. Premkumar, D. K. Joseph and K. E.Geckeler, *React. Funct. Polym.*, 2007, **67**, 844-858.

1 44. H. Yang, W. Wang and A. Wang, *J. Disper. Sci. Technol.*, 2012, **33**, 1154-1162.

2

Figure captions

Scheme 1 Chemical structure of NaAlg.

Scheme 2 Proposed mechanism of the formation of NaAlg-g-PAA/organo-loess (loess) superabsorbent composite.

Fig. 1. FTIR spectra of (a) loess and (b) organo-loess.

Fig. 2. FTIR spectra of (a) NaAlg, (b) NaAlg-g-PAA, (c) NaAlg-g-PAA/loess and (d) NaAlg-g-PAA/organo-loess.

Fig. 3. Scanning electron micrographs of (a) NaAlg-g-PAA, (b) NaAlg-g-PAA/loess and (c) NaAlg-g-PAA/organo-loess.

Fig. 4. Element mapping of the NaAlg-g-PAA/organo-loess.

Fig. 5. XRD spectra of the (a) loess, (b) organo-loess, (c) NaAlg-g-PAA/loess and (d) NaAlg-g-PAA/organo-loess.

Fig. 6. TGA spectra of superabsorbent composites.

Fig. 7. DSC spectra of superabsorbent composites

Fig. 8. Effect of loess content in the superabsorbent composites on water absorbencies: (a) NaAlg-g-PAA/loess and (b) NaAlg-g-PAA/organo-loess composite in distilled water; (c) NaAlg-g-PAA/loess and (d) NaAlg-g-PAA/organo-loess composite in 0.9 wt% NaCl solution.

Fig. 9. Effect of MBA amount on the on water absorbencies.

Fig. 10. Water absorbencies of superabsorbent composites as a function of pH values.

Fig. 11. Equilibrium swelling capacity of the superabsorbent composites in (a) NaCl

solutions, (b) $CaCl_2$ and (c) $FeCl_3$ solutions with various concentration.

Fig. 12. Effect of different surfactants on water absorbency of superabsorbent composites: (a) NaAlg-g-PAA/loess and (b) NaAlg-g-PAA/organo-loess composite in various concentrations SDBS solution; (c) NaAlg-g-PAA/loess and (d) NaAlg-g-PAA/ organo-loess composites in various concentrations CTAB solution.

Fig. 13. Water retention of the swollen samples as a function of time at 60 and 100 ^{o}C, respectively.

Scheme 1

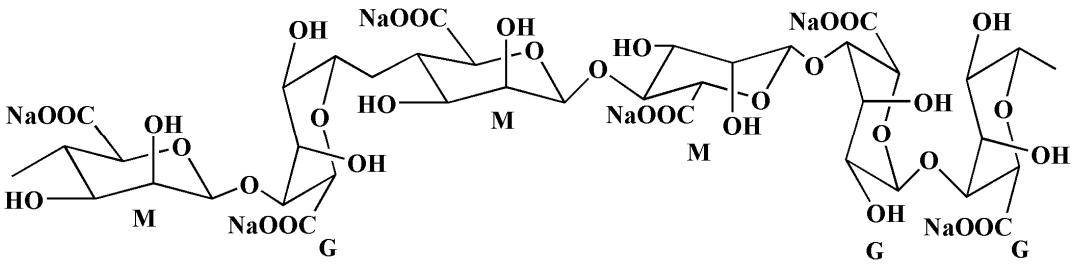

Scheme 2

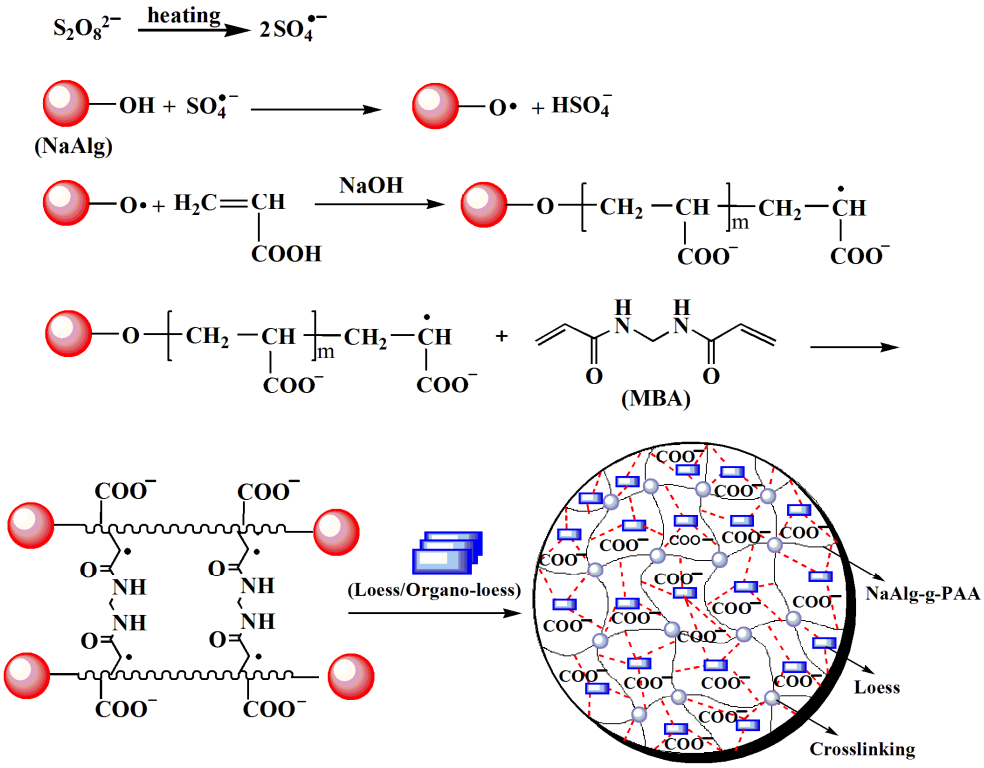

Fig. 1

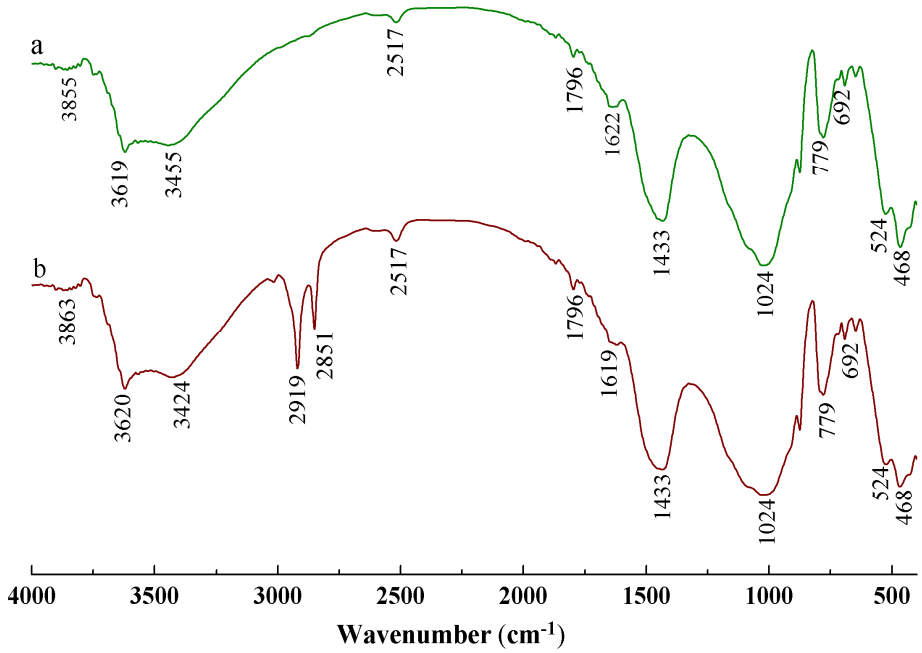

Fig. 2

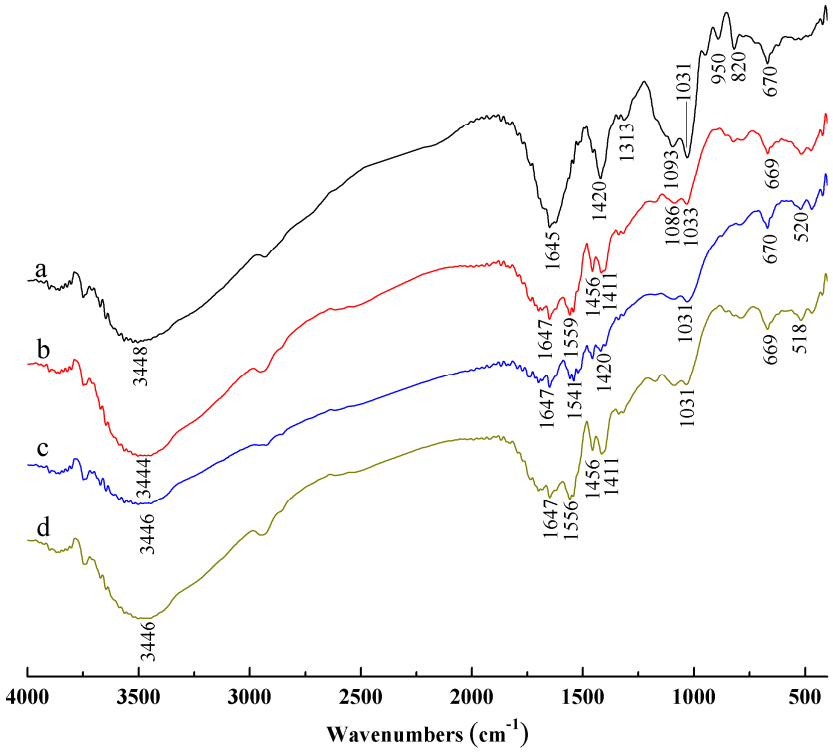

Fig. 3

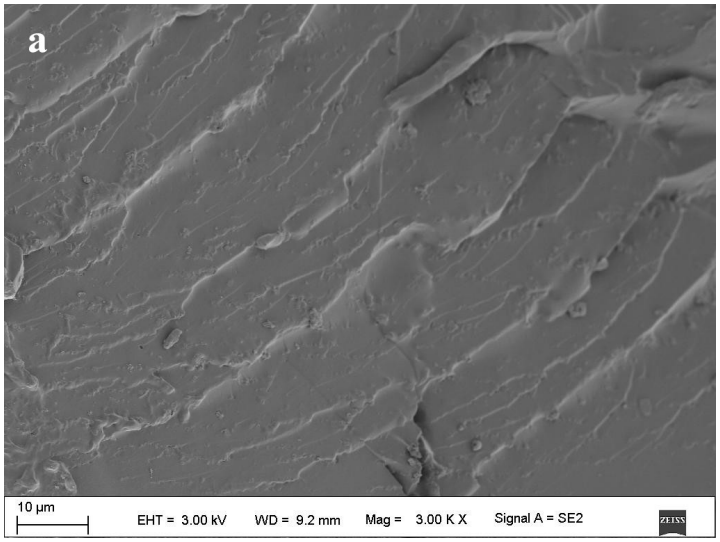

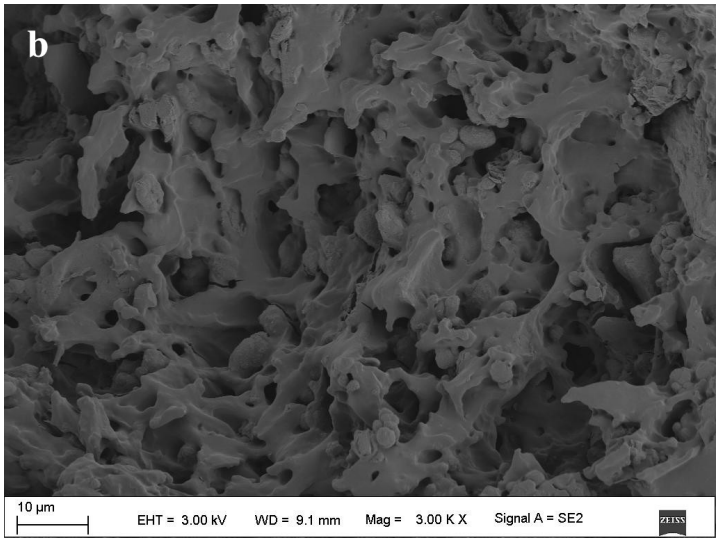

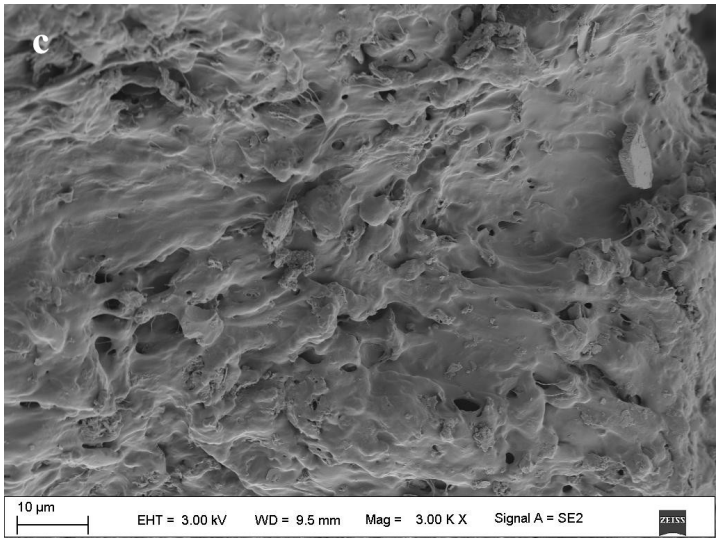

Fig. 4

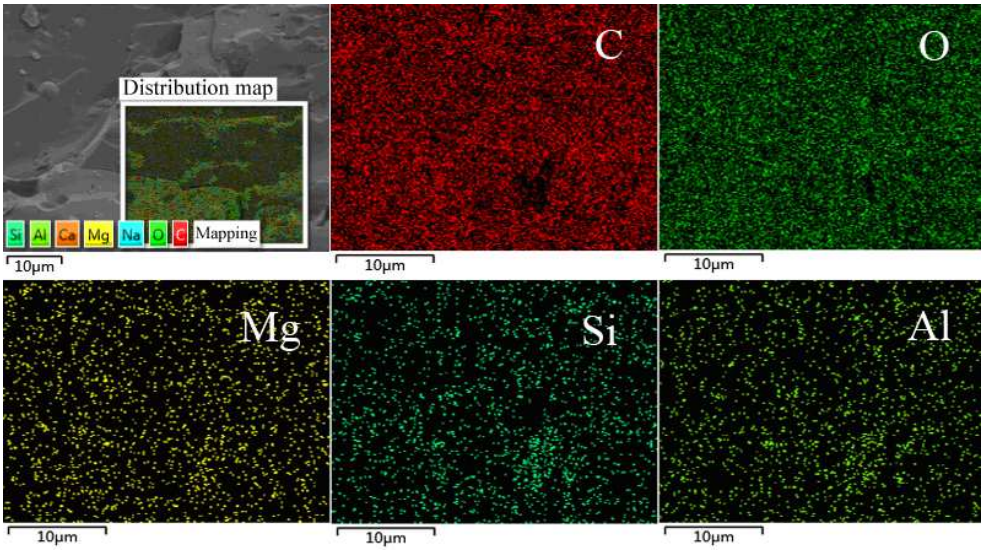

Fig. 5

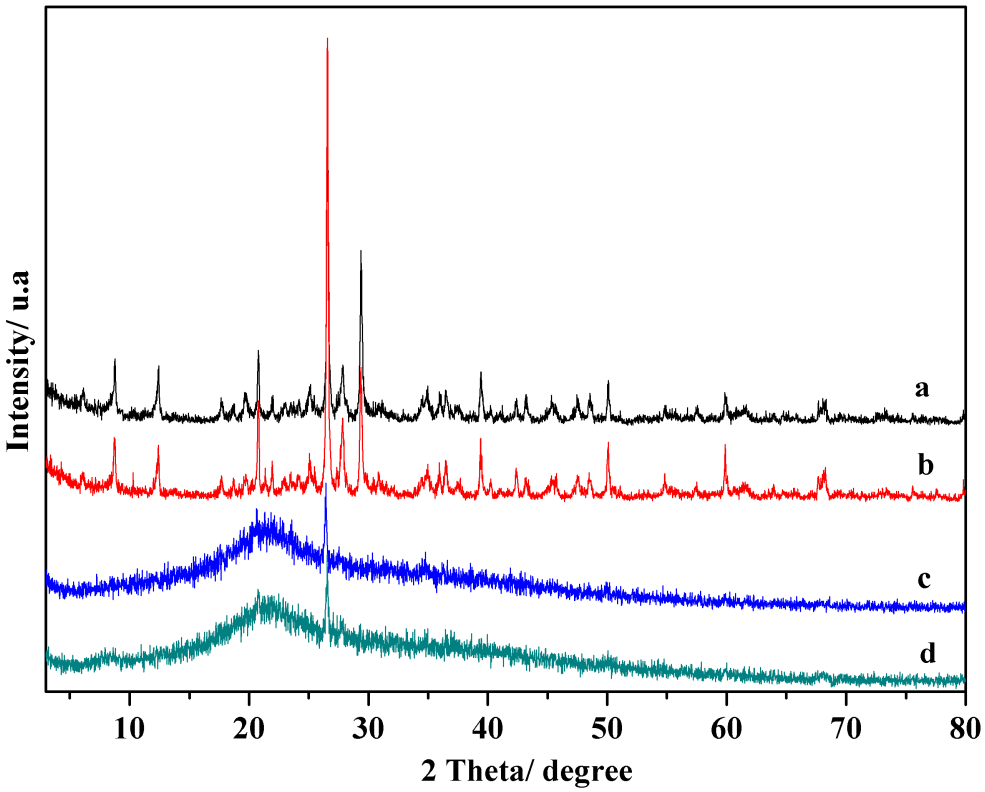

Fig. 6

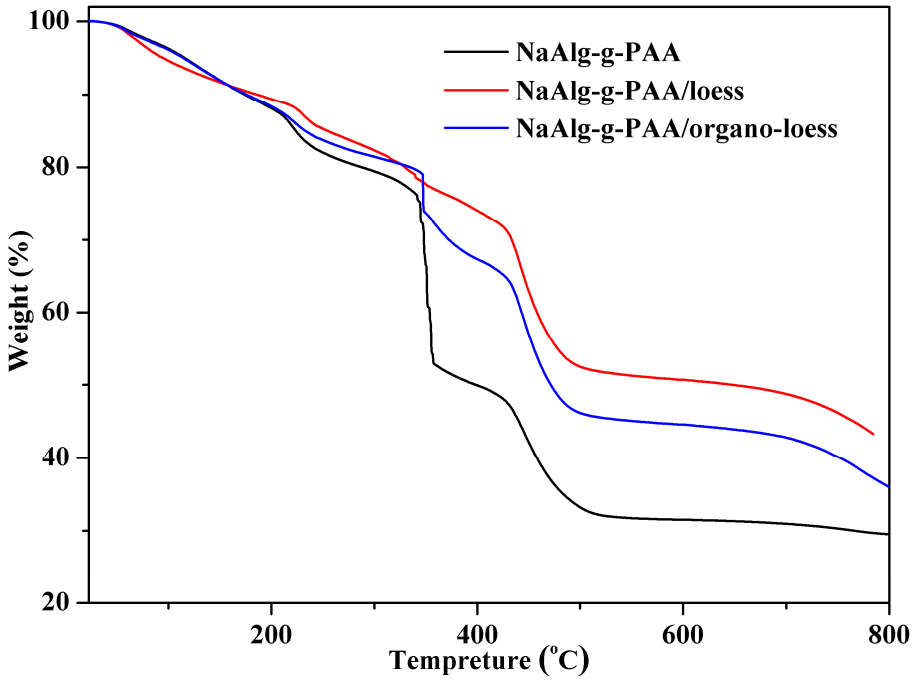

Fig. 7

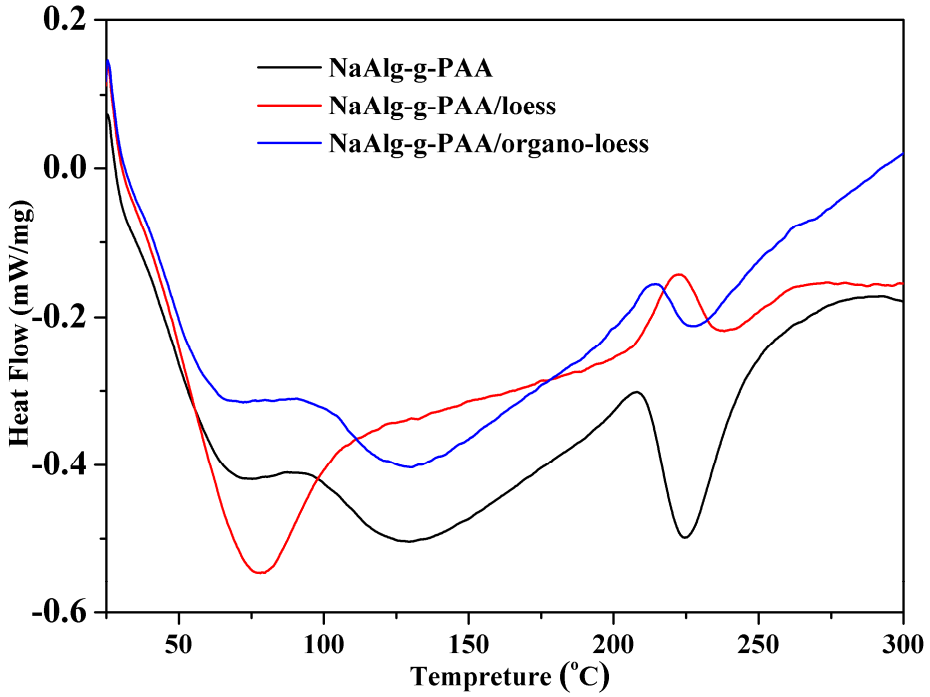

Fig. 8

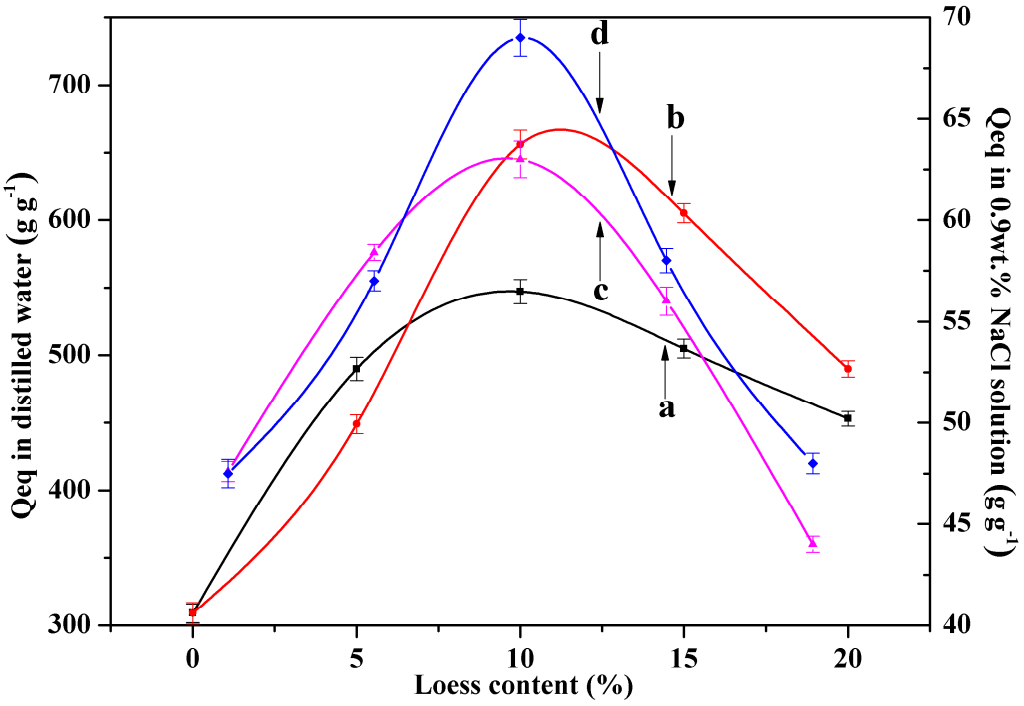

Fig. 9

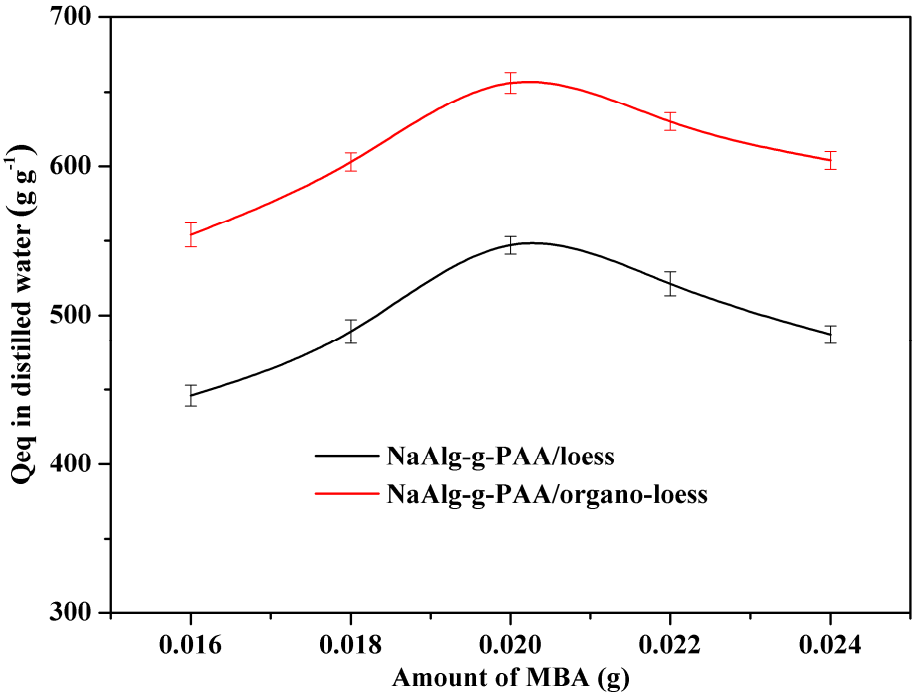

Fig. 10

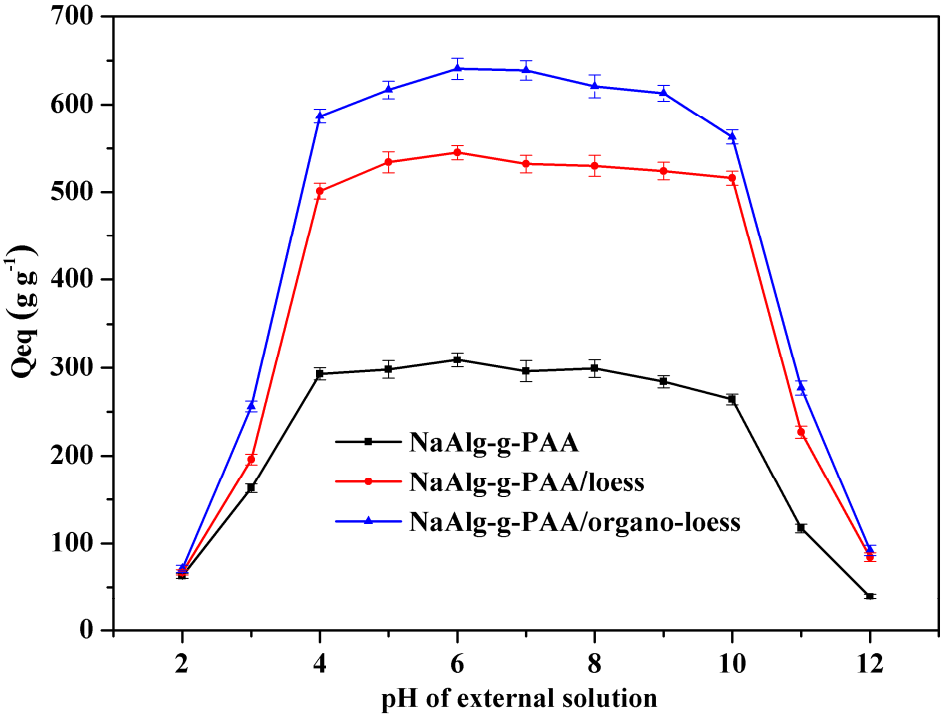

1 Fig. 11

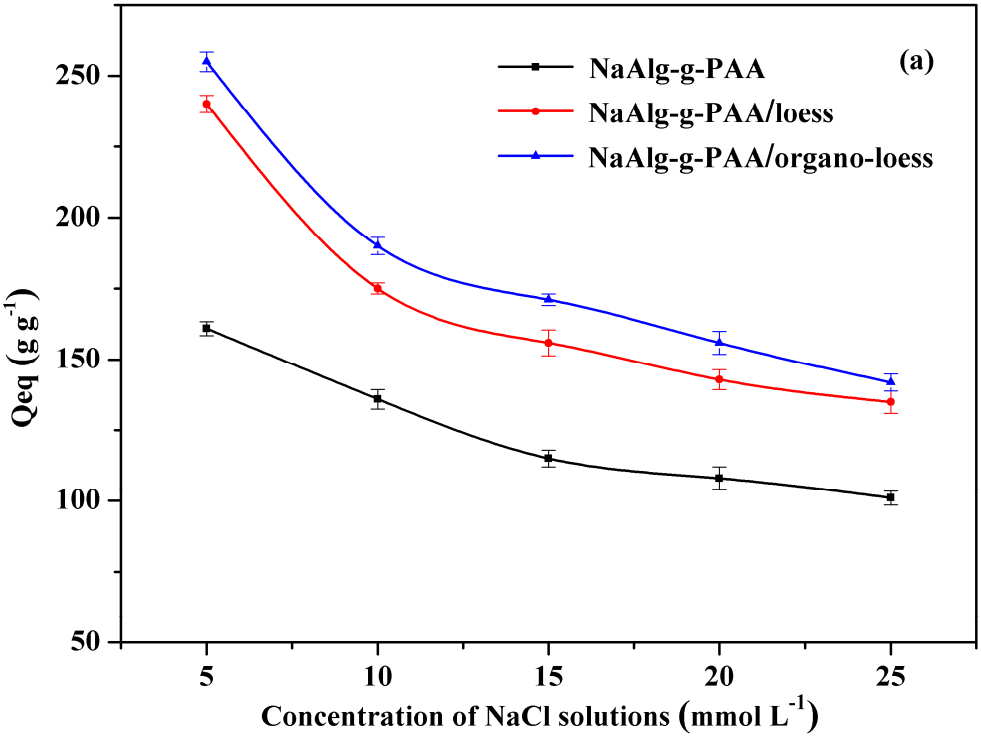

2

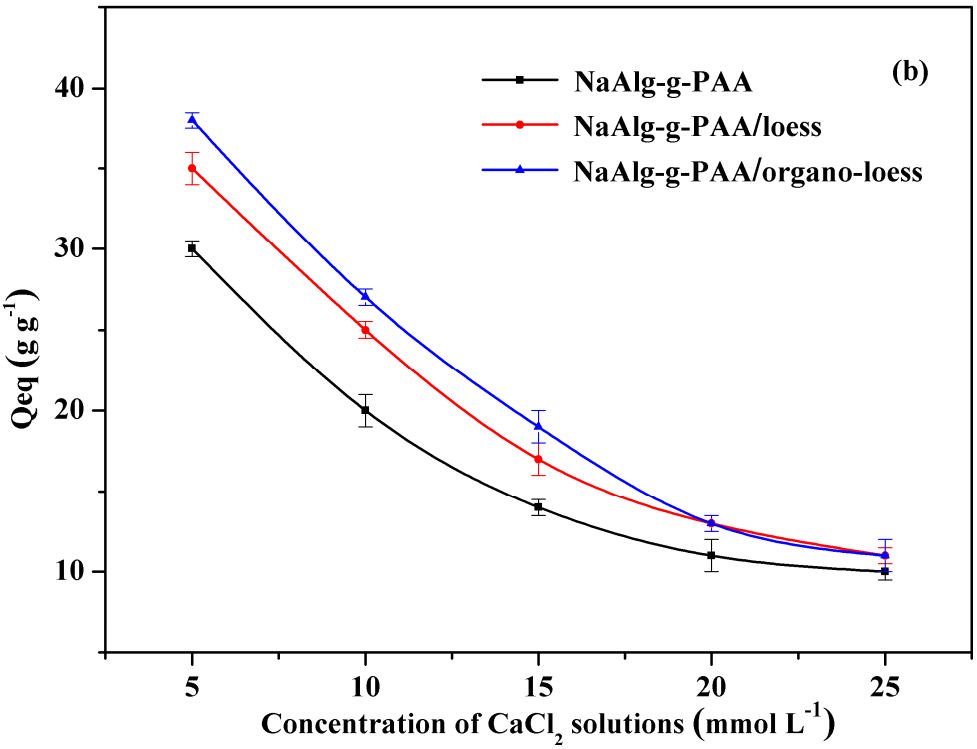

3

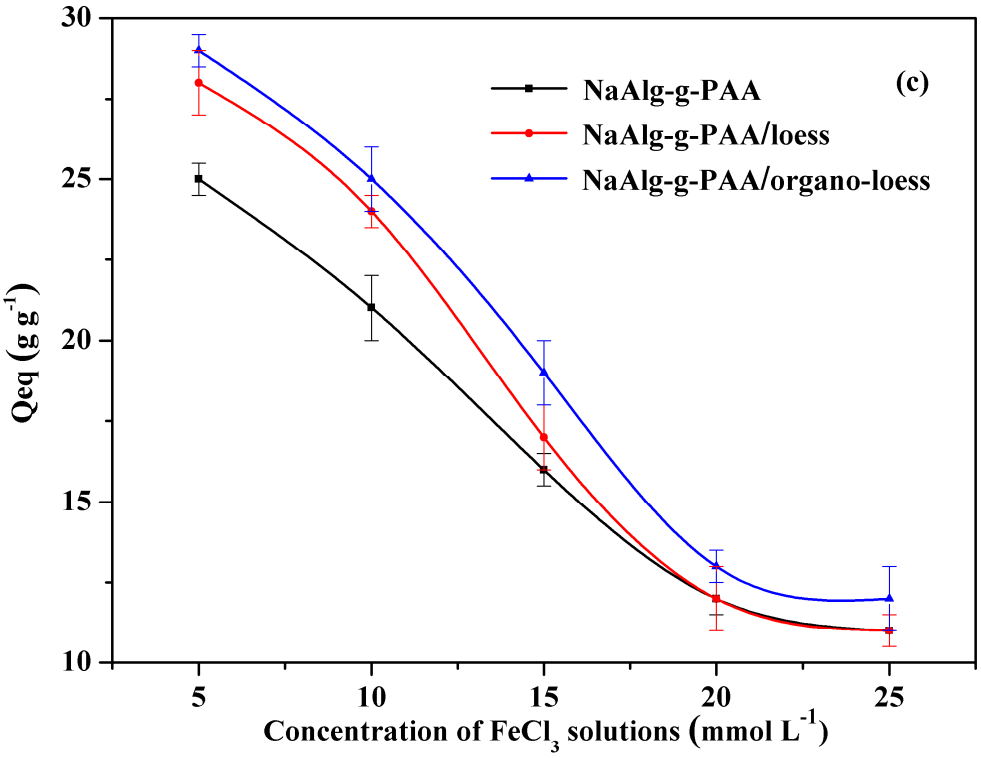

Fig. 12

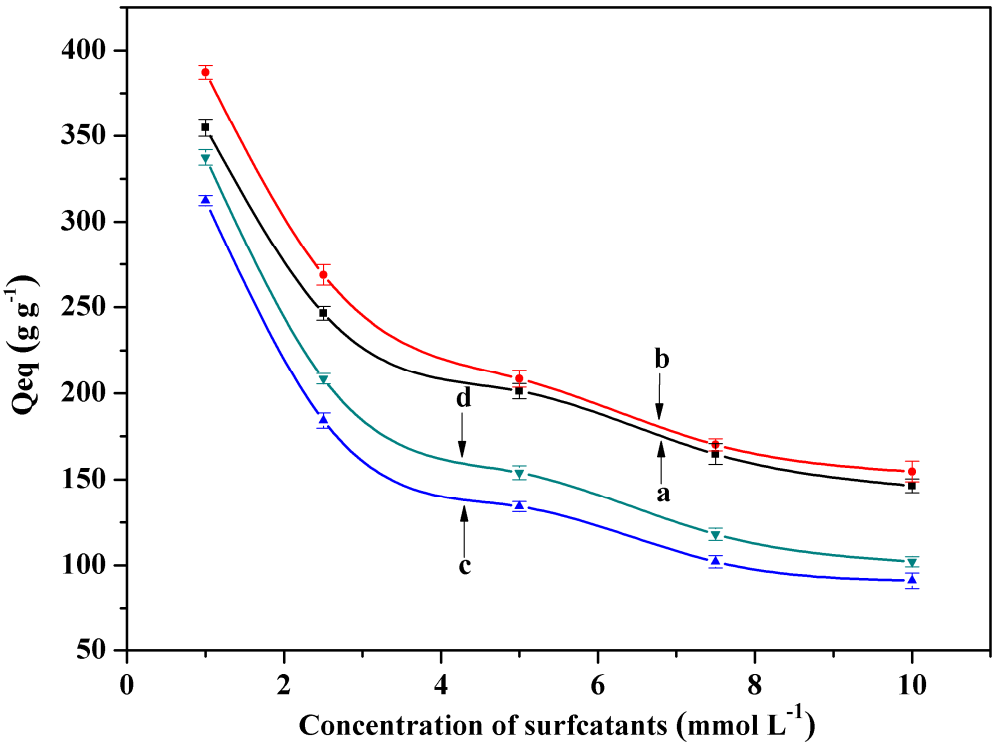

1 Fig. 13

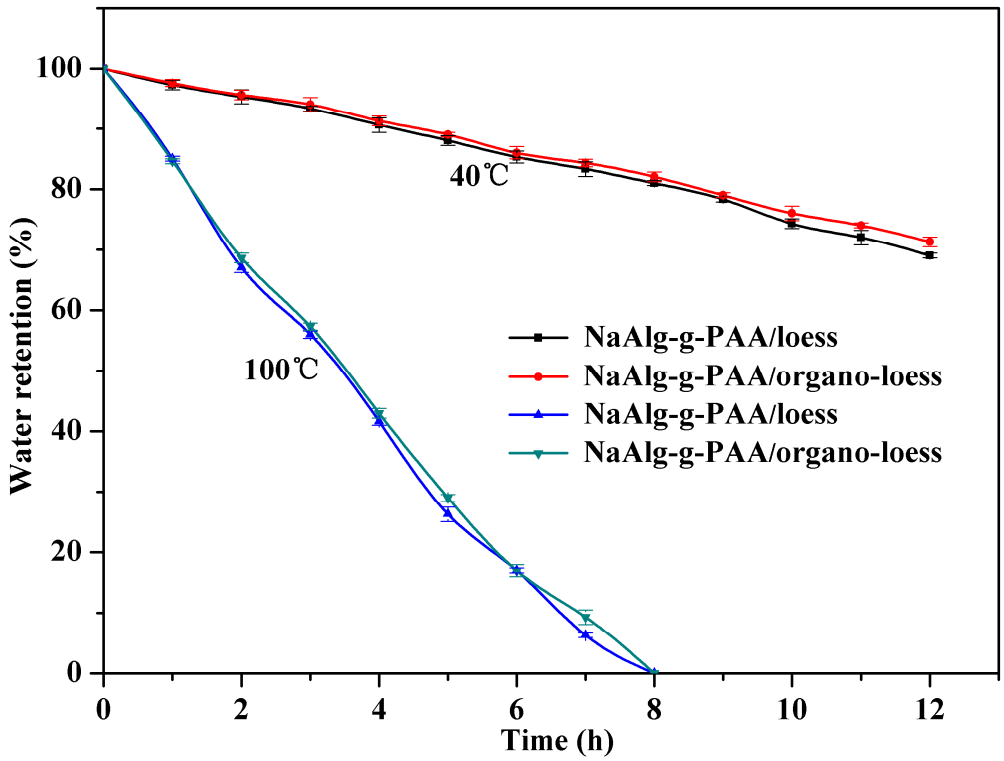

2
3
4
5
6
7
8
9
10
11
12
13